An interval power flow for unbalanced distribution systems based on the Three-Phase Current Injection Method

Heitor M. Rodrigues Junior [a,*], Igor D. Melo [a], Erivelton G. Nepomuceno [b]

[a] *Federal University of Juiz de Fora, Juiz de Fora, Brazil*
[b] *Maynooth University, Maynooth, Ireland*

A B S T R A C T

Interval arithmetic has been widely used for power systems analysis considering uncertainties associated with load and generation data. However, little work can be found within the context of three-phase distribution systems due to their peculiarities such as radial topology and unbalanced loads. In this paper, a novel methodology is proposed for determining interval results of a power system load flow for three-phase unbalanced distribution networks based on the Three-Phase Current Injection Method (TPCIM) in which state variables are considered in rectangular coordinates. In the proposed approach, active and reactive powers at each load bus are modelled as interval values to represent their inherent uncertainties and the Krawczyk operator is applied into the power flow equations in order to provide reliable interval three-phase results. Additionally, the use of interval extensions and an angular rotation technique are proposed to overcome overestimation problems associated with the interval solutions. Computational simulations are carried out using IEEE 13, 33 and 69-bus test systems. The main contribution of this work is the proposition of two methods based on traditional interval arithmetic to reduce the diameter of the solution and achieve similar results when compared with Affine Arithmetic and Monte Carlo Simulations. Additionally, the computational time associated with the algorithm is extremely advantageous. The method is useful for power distribution systems operation and planning studies, representing a viable and useful tool for calculating the impact of uncertain input data on the power flow results.

1. Introduction

Due to ever increasing use of renewable energy resources based on green technologies, such as solar and wind farms, uncertainties associated with generation have been increased enormously. Additionally, new types of loads such as electric vehicles and power electronic devices, are also being inserted into power systems rising the uncertainties over the energy demand values [1–3]. Within this challenging scenario, new developments based on the traditional power flow equations must be investigated and proposed for reliable power systems operation and planning.

Distribution systems are generally associated with inherent characteristics such as radial or weakly-meshed topology and overhead lines with shorter distances when compared to transmission systems. Moreover, differently from the high voltage networks, some distribution feeders are not monitored in real time due to a few number of installed measurement units allocated along the systems [4]. Additionally, daily load variations and the insertion of intermittent distributed generation rise the uncertainty levels associated with active and reactive powers.

To tackle this important issue, probabilistic methods are often used within this context [5–7], being the Monte Carlo Simulations (MCS) one of the most widely known methods for computing the stochasticity of the variables associated to power flow solutions. One of the biggest disadvantages is the associated computational time to determine satisfactory results which are generally defined as an interval number with lower and upper bounds according to the uncertainty level of the input variables. Even using supercomputers, the time spent in the analysis of uncertainties in power flow with MCS can be high, being proportional to the amount of pre-determined simulations and the complexity of the electrical system. In this context, fuzzy-based methods are also proposed to incorporate uncertain parameters as input data for power flow algorithms [8–10].

Interval power flows are commonly used in the literature in order to obtain interval results for voltage magnitudes and angles assuming uncertainties over demand and generation data [11–13]. Despite the lower computational burden, one of the major challenge is to determine

---

interval results which accommodate the ones obtained by MCS, meaning that the interval solutions must be larger than the ones obtained by MCS. On the other hand, overestimation must be avoided in order not to obtain extremely larger intervals compromising the accuracy of the results. There are several interval approaches proposed to reduce overestimation caused by the traditional interval load flow algorithms, such as the application of Affine Arithmetic [14] and the use of Taylor series [15].

Krawczyk operator is used in some references based on the application of the interval and Affine Arithmetic (AA) into the Current Injection Method (CIM) presented in [16]. Based on this reference, [17] proposes the incorporation of traditional interval arithmetic in the solution of single-phase power flow using CIM. Ref. [18] proposes the incorporation of AA in the formulation of single-phase power flow using the CIM and an interval power flow is proposed in [19] based on the CIM for evaluating symmetrical and asymmetrical faults. In these methodologies, the load flow solution is obtained using rectangular coordinates as state variables to be determined iteratively by Newton–Raphson and only single-phase systems with meshed topology are used in the case studies.

An interval load flow based on the three-phase implementation of backward/forward sweep method is presented in [20–22]. Results accommodate the MCS being suitable for applications considering uncertain variables in power systems. However, based on the literature review, there is no paper considering the Three-Phase Current Injection Method (TPCIM) in order to represent distribution systems with radial topology including intrinsic characteristics such as uncertain input data, mutual impedances and unbalanced loads.

In this paper, the TPCIM equations are used to determine the power flow solution of unbalanced distribution networks. Assuming uncertainties over active and reactive powers, the Krawczyk operator is used to determine intervals for voltage magnitudes and angles at each system bus. Uncertainties are modelled using interval arithmetic. Comparative analysis using different evaluation indices are performed for each case study being the simulations carried out using IEEE 13, 33 and 69-bus test systems. Results are compared with MCS to demonstrate the viability and efficiency of the proposed method.

The main contributions of this paper include the following: (i) a novel methodology is proposed to determine three-phase voltage intervals using the Three-Phase Current Injection Method (TPCIM); (ii) three-phase voltage phasors are obtained with reduced intervals using interval extensions concept and angular rotation techniques; (iii) interval results can be obtained in an advantageous computational time when compared with Monte Carlo simulations.

This paper is divided into five main sections including this introductory one. In the second section, the proposed methodology is presented including a brief review of interval arithmetic, the deterministic TPCIM equations and the application of Krawczyk operator into the power flow equations. In the third one, results of the computational simulations are presented and discussed. Finally, conclusions are highlighted in the last section.

2. Proposed methodology

The proposed methodology is described in this section, including the representation of uncertain variables using interval arithmetic, the deterministic TPCIM equations and the application of Krawczyk operator into the power flow equations to determine three-phase results.

2.1. Interval arithmetic

From a simple numerical model, each variable in the real numbers domain can be represented by numerical intervals, being possible to perform addition, subtraction, multiplication and division operations in such a way that each computed interval contains the unknown value of the associated variable.

According to Refs. [23] and [24], an interval X can be defined as a closed and limited set of real numbers, $x \in \mathbb{R}$, according to Eq. (1) in which $\underline{x}$ and $\overline{x}$ are the lower and upper bounds of the interval variable, respectively.

$$X = [\underline{x}, \overline{x}] = \{x : \underline{x} \leq x \leq \overline{x}\} \tag{1}$$

The size $\omega(X)$ and midpoint, $m(X)$ of a given interval are defined by Eqs. (2) e (3), respectively.

$$\omega(X) = \overline{x} - \underline{x} \tag{2}$$

$$m(X) = \frac{\underline{x} + \overline{x}}{2} \tag{3}$$

The intersection between two intervals X and Y is empty if $\overline{y} < \underline{x}$ or $\overline{x} < \underline{y}$ being denoted by $X \cap Y = \emptyset$. Otherwise, the intersection between X and Y is the interval obtained by Eq. (4).

$$X \cap Y = [max\{\underline{x}, \underline{y}\}, min\{\overline{x}, \overline{y}\}] \tag{4}$$

The basic interval operations associated with addition, subtraction and multiplication are respectively defined by Eq. (5), (6), (7) and (8) where $S = \{\underline{x} \cdot \underline{x}, \underline{x} \cdot \overline{y}, \overline{x} \cdot \underline{y}, \overline{x} \cdot \overline{y}\}$.

$$X + Y = \left[\underline{x} + \underline{y}, \overline{x} + \overline{y}\right] \tag{5}$$

$$X - Y = \left[\underline{x} - \overline{y}, \overline{x} - \underline{y}\right] \tag{6}$$

$$X \cdot Y = [min\{S\}, max\{S\}] \tag{7}$$

$$\frac{X}{Y} = X \cdot \frac{1}{Y} \tag{8}$$

According to [25], it is also possible to affirm that the size of the intersection between two intervals X and Y is, at most, the smallest of the intervals as described by Eq. (9).

$$\omega(X \cap Y) \leq min\{\omega(X), \omega(Y)\} \tag{9}$$

Other basic operations are detailed in Ref. [23,24].

2.2. The proposed Interval Three-Phase Current Injection Method

The proposed Interval Three-Phase Current Injection Method (IT-PCIM) is developed based on the deterministic results of the Three-Phase Current Injection Method (TPCIM) [26], formulated in terms of nodal voltages in rectangular coordinates. The main advantages of the usage of the TPCIM include fast convergence process and robustness to calculate electrical variables in three-phase power distribution systems considering unbalanced loads and mutual impedances. Additionally, the elements out of the diagonal of the Jacobian matrix remains constant during the iterative process for determining the solution via Newton–Raphson being the method described in detail in this work in Appendix A.

Load uncertainties associated with active and reactive powers are modelled in ITPCIM as presented in Eqs. (10) and (11), respectively.

$$P_{D_k}^{s,i} = [P_{D_k}^{s,d} \cdot (1 - \alpha_{P_k}^s), P_{D_k}^{s,d} \cdot (1 + \alpha_{P_k}^s)], \qquad \alpha_{P_k}^s \in \{0, 1\} \tag{10}$$

$$Q_{D_k}^{s,i} = [Q_{D_k}^{s,d} \cdot (1 - \alpha_{Q_k}^s), Q_{D_k}^{s,d} \cdot (1 + \alpha_{Q_k}^s)], \qquad \alpha_{Q_k}^s \in \{0, 1\} \tag{11}$$

where $P_{D_k}^{s,i}$ and $Q_{D_k}^{s,i}$ are the intervals associated with active and reactive powers demanded at bus k for a given phase s, respectively. The $\alpha_{P_k}^s$ and $\alpha_{Q_k}^s$ factors denote the corresponding active and reactive load percentage uncertainties.

Other variables with an associated level of uncertainty can be analogously described.

The initialisation of the interval voltage profile is defined by the mean of the interval radius of these voltages which is calculated by Eq. (12):

$$\begin{bmatrix} \Delta \mathbf{V}_{re}^{s,i} \\ \Delta \mathbf{V}_{im}^{s,i} \end{bmatrix} = (\mathbf{J}^d)^{-1} \begin{bmatrix} \Delta \mathbf{I}_{im}^{s,i} \\ \Delta \mathbf{I}_{re}^{s,i} \end{bmatrix} \tag{12}$$

where $\mathbf{J}^d$ is the Jacobian matrix associated with the deterministic power flow. The vectors $\Delta \mathbf{I}_{re}^{s,i}$ and $\Delta \mathbf{I}_{im}^{s,i}$ are composed of real and imaginary components of interval current residuals at each phase s as described by Eqs. (13) and (14), respectively:

$$\Delta I_{re_k}^{s,i} = I_{re_k}^{s,d} - \frac{(P_{G_k}^{s,i} - P_{D_k}^{s,i}) \cdot V_{re_k}^{s,d} + (Q_{G_k}^{s,i} - Q_{D_k}^{s,i}) \cdot V_{im_k}^{s,d}}{(V_k^{s,d})^2} \tag{13}$$

$$\Delta I_{im_k}^{s,i} = I_{im_k}^{s,d} - \frac{(P_{G_k}^{s,i} - P_{D_k}^{s,i}) \cdot V_{im_k}^{s,d} + (Q_{G_k}^{s,i} - Q_{D_k}^{s,i}) \cdot V_{re_k}^{s,d}}{(V_k^{s,d})^2} \tag{14}$$

where $V_k^{s,d} = V_{re_k}^{s,d} + jV_{im_k}^{s,d}$ and $I_k^{s,d} = I_{re_k}^{s,d} + jI_{im_k}^{s,d}$ are the voltage and current injected at bus k for a given phase s; $P_{G_k}^{s,i}$ and $Q_{G_k}^{s,i}$ are the active and reactive power generation at bus k.

From the voltage interval radius presented in Eq. (12), the real and imaginary parts of the voltage intervals can be initialised as presented by Eqs. (15) and (16), respectively:

$$V_{re_k}^{s,i} = V_{re_k}^{s,d} + \overline{\Delta V_{re_k}^{abc,i}} \tag{15}$$

$$V_{im_k}^{s,i} = V_{im_k}^{s,d} + \overline{\Delta V_{im_k}^{abc,i}} \tag{16}$$

where $\overline{\Delta V_{re_k}^{abc,i}}$ and $\overline{\Delta V_{im_k}^{abc,i}}$ represent the mean value of the interval radius obtained for a bus k for the three phases being the real and imaginary parts presented by Eqs. (17) and (18) respectively. This feature ensures the initialisation of the voltages for a given bus k with intervals of same width for the three phases.

$$\overline{\Delta V_{re_k}^{abc,i}} = \frac{V_{re_k}^{a,i} + V_{re_k}^{b,i} + V_{re_k}^{c,i}}{3} \tag{17}$$

$$\overline{\Delta V_{im_k}^{abc,i}} = \frac{V_{im_k}^{a,i} + V_{im_k}^{b,i} + V_{im_k}^{c,i}}{3} \tag{18}$$

Based on these deterministic results provided by the traditional TPCIM, the iterative Krawczyk methodology is used in order to determine the three phase interval solution. Within the context of the interval arithmetic, the Krawczyk operator allows to determine the solution not being necessary to calculate the inverse of the Jacobian matrix which would result in oversized intervals. For a given iteration h of the Krawczyk method, the operator is applied according to Eq. (19):

$$K\left(\mathbf{x}^{(h)}, \mathbf{X}^{(h)}\right) = \mathbf{x}^{(h)} - \mathbf{C}f\left(\mathbf{x}^{(h)}\right) + \left[\mathbf{I} - \mathbf{C}\mathbf{J}\left(\mathbf{X}^{(h)}\right)\right]\left(\mathbf{X}^{(h)} - \mathbf{x}^{(h)}\right) \tag{19}$$

where $\mathbf{x}^{(h)}$, $\mathbf{X}^{(h)}$ and $f(\mathbf{x}^{(h)})$ are determined by Eqs. (20), (21) and (22), respectively. $\mathbf{J}(\mathbf{X})$ is the Jacobian matrix calculated for the interval vector $\mathbf{X}$, $\mathbf{C}$ is a preconditioning matrix given by the inverse of the midpoint of $\mathbf{J}(\mathbf{X})$ and $\mathbf{I}$ is the identity matrix.

$$\mathbf{x}^{(h)} = \begin{bmatrix} \mathbf{V}_{re}^{s,d} \\ \mathbf{V}_{im}^{s,d} \end{bmatrix} \tag{20}$$

$$\mathbf{X}^{(h)} = \begin{bmatrix} \mathbf{V}_{re}^{s,i} \\ \mathbf{V}_{im}^{s,i} \end{bmatrix} \tag{21}$$

$$f(\mathbf{x}^{(h)}) = \begin{bmatrix} \Delta \mathbf{I}_{re}^{s,i} \\ \Delta \mathbf{I}_{im}^{s,i} \end{bmatrix} \tag{22}$$

The solution of the nonlinear system is achieved by the intersection between the interval sets $\mathbf{X}^{(h)}$ and $K\left(\mathbf{x}^{(h)}, \mathbf{X}^{(h)}\right)$ as presented in Eq. (23). The iterative process converges when the difference between the radius of all elements of $\mathbf{X}$ at iterations h and $h+1$ is less than a specified tolerance τ, which is generally 10^{-6}.

$$\mathbf{X}^{(h+1)} = \mathbf{X}^{(h)} \cap K\left(\mathbf{x}^{(h)}, \mathbf{X}^{(h)}\right) \tag{23}$$

Table 1
Example of the use of interval extensions.

Variables	Value	F_1	F_2	$F_1 \cap F_2$
P_k^{sch,a^i}	[0.4,0.5]			
Q_k^{sch,a^i}	[0,0.2]			
$V_{re_k}^{a,i}$	[0.9,1.1]	[0.1407,1.0563]	[0.1407,1.2026]	[0.1407,1.0563]
$V_{im_k}^{a,i}$	[−0.2,0.2]			

2.2.1. Use of interval extensions

For a given function f defined for a real variable x, a interval extension of f is an interval function F defined for an interval variable X, such that for real arguments $F(X) = f(x)$.

As stated in Eq. (9), the use of the intersection of interval extension solutions can be used as a tool to reduce the size of the interval obtained as a solution of a given function. Thus, interval extensions are applied to the partial derivative equations of the interval Jacobian matrix, detailed in Appendix A.

For instance, the term of the interval Jacobian matrix related to the partial derivative of the real component of the current injection in the phase a for a bus k with respect to the real voltage component associated with the same phase for the same bus can be described by the Eqs. (24) and (25) in which F_1 and F_2 represent the corresponding interval extensions.

$$F_1 = \frac{\partial I_{re_k}^{a,i}}{\partial V_{re_k}^{a,i}} = \frac{P_k^{sch,a^i} \cdot \left[\left(V_{re_k}^{a,i}\right)^2 - \left(V_{im_k}^{a,i}\right)^2\right] + 2 \cdot V_{re_k}^{a,i} \cdot V_{im_k}^{a,i} \cdot Q_k^{sch,a^i}}{\left(V_k^{a,i}\right)^4} \tag{24}$$

$$F_2 = \frac{\partial I_{re_k}^{a,i}}{\partial V_{re_k}^{a,i}}$$

$$= \frac{P_k^{sch,a^i} \cdot \left[\left(V_{re_k}^{a,i}\right) \cdot \left(V_{re_k}^{a,i}\right) - \left(V_{im_k}^{a,i}\right)\left(V_{im_k}^{a,i}\right)\right] + 2 \cdot V_{re_k}^{a,i} \cdot V_{im_k}^{a,i} \cdot Q_k^{sch,a^i}}{\left(V_k^{a,i}\right)^2 \cdot \left(V_k^{a,i}\right)^2} \tag{25}$$

In order to prove the importance of the use of the interval extensions concept to obtain reduced intervals, Table 1 presents random values for the variables associated with the active/reactive powers and real/imaginary parts of the voltage magnitudes at a given bus k ($P_k^{sch,a^i}, Q_k^{sch,a^i}, V_{re_k}^{a,i}, V_{im_k}^{a,i}$, respectively). It can be noted that, based on simple interval values, the calculation of F_1 and F_2 result in different intervals. Note that, when the intersection of these results is considered, at least, the interval solution with the smallest width is obtained as a consequence.

Although the use of interval extensions is traditional in the interval arithmetic context according to [23], this concept is being used in this paper in order to effectively reduce the intervals associated with the solution obtained using a Three-Phase Current Injection Method for determining the load flow in unbalanced distribution systems.

2.2.2. Use of angular rotation

In the application of Krawczyk operator in the three-phase load flow it is observed that there are differences in the resulting intervals, mainly between phase A and the others. One of the possible reasons for these differences is the angular position of the voltages obtained with deterministic flow, mainly due to the fact that the voltages in phases B and C would, in general, be displaced by about 120° and 240° respectively, making the rectangular forms of these voltages have the absolute values of the real and imaginary terms very close. For example, two complex numbers with unitary magnitude, respectively displaced on the Cartesian plane of 120° and 240°, would be $-0.5 + j0.87$ and $-0.5 - j0.87$ in rectangular form.

In order to reduce the interference of software issues related to the treatment of complex interval variables, a strategy is developed
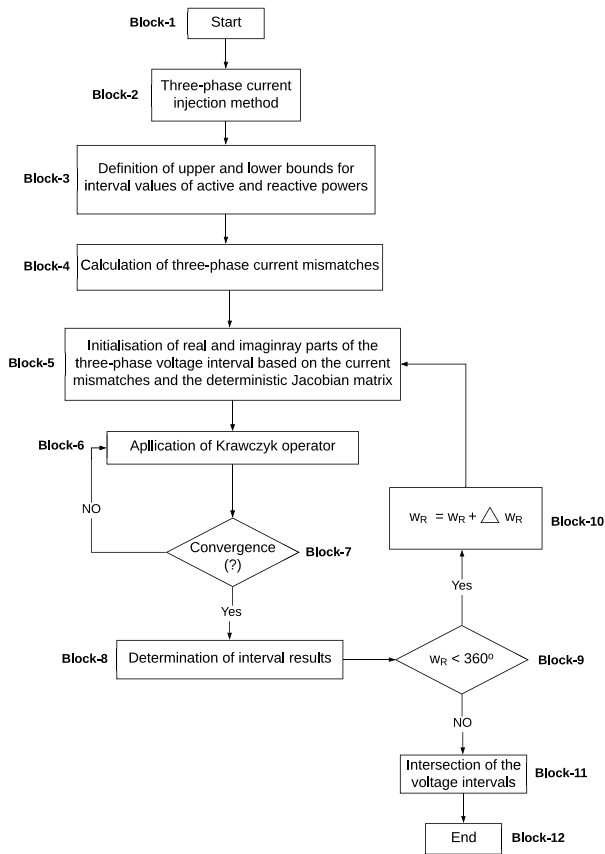
Fig. 1. Flowchart of the proposed methodology.

to obtain different solutions rotating the voltage phasors by the same angular displacement in the three phases. Thus, with each displacement of the phasors, the magnitude and the angular difference between the voltages in the three phases would remain, causing no characteristic to be altered in the power flow problem.

After completing 360 degrees executing the desired number of rotations by some angular displacement ω_R, the interval voltages obtained at each angular displacement must be intersected. It is important to mention that the resulting voltages at the end of each step must be rotated back to the starting position to obtain its angles. The resulting interval is expected to contain the true solution and be at least the width of the smallest intersected interval.

2.2.3. Solution methodology

A flowchart of the proposed methodology is presented in Fig. 1 divided into blocks to be explained in detail.

- Block-1: This block indicates the initialisation of the algorithm. The nominal loads, impedances of the distribution lines, DG data are considered as variables to be used in a deterministic load flow program. Initial values associated with the three-phase voltage phasors are $1\underline{/0°}$, $1\underline{/120°}$, $1\underline{/-120°}$ for phases A, B and C, respectively;
- Block-2: Based on the input data and initial values determined as previously mentioned, three-phase voltages are calculated according to the Three-Phase Current Injection method;
- Block-3: The interval limits are determined for the active and reactive loads by Eqs. (10) and (11) respectively. Additionally, if uncertain data associated with generation are considered for the computational simulations, they can be determined analogously;
- Block-4: The current mismatches are calculated as presented in Eqs. (13) and (14);

- Block-5: This block indicates the initialisation of the interval voltages, which are according to Eqs. (15) and (16);
- Block-6: In this block, the Krawczyk operator is applied according to Eq. (19) and the convergence is verified for a predefined tolerance value, τ;
- Block-7: If the convergence $\tau = 10^{-6}$ is not achieved in a single iteration, the Krawczyk operator is applied again into the power flow equations iteratively until the tolerance is satisfied;
- Block-8: The three-phase voltage intervals are obtained, as indicated by Eq. (23) considering the three voltage phasors, separated by 120 degrees;
- Block-9: Once the voltage angles for each one of the three phases will be modified according to the procedure described in Section 2.2.2, it is necessary to verify if the angular rotation is less than 360 degrees. Note that the complete solution is only determined after the angular displacement completes 360 degrees in a trigonometric cycle;
- Block-10: This block indicates the application of the angular rotation methodology in which the voltage angles are modified considering $\pm120°$ increments in the initial values adopted for the load flow program analysis;
- Block-11: This block indicates the calculation of the intersection of the voltage intervals obtained at each rotation in order to ensure that the interval solution associated with the smallest width are obtained;
- Block-12: This block indicates the end of the algorithm.

3. Results and discussion

In this section, the applicability of the complete interval methodology developed in the work is carried out. This analysis is based on the comparison of the interval voltages obtained with ITPCIM and the ranges of possible values obtained with MCS. Therefore, it is expected that the intervals resulting from the developed methodology encompass these values obtained with the probabilistic method. After that, evaluations of the proposed improvements are made with the use of interval extensions and the angular rotation technique. The results show that the widths of ITPCIM solutions are much tighter with these improvements. The interval voltages resulting from the application of ITPCIM will be evaluated in three different unbalanced distribution systems and a case study considering the insertion of distributed generation (DG) will be analysed. All assessments will be carried out based on pre-established indexes in the literature. It is important to mention that 100,000 trials are performed in each MCS application. For the MC simulations, an uniform probability density function is associated with the uncertain variables.

To analyse the applicability of ITPCIM and compare the proposed improvements, IEEE 69-bus distribution system is used as case study. Fig. 2 presents the single line diagram of this test system. This 12.66 kV network is composed of 68 load buses and the substation is the bus 69. More details about load and line data can be obtained in [27]. In order to consider an unbalanced case study, the nominal load data is multiplied by a factor equal to 1.0, 0.8 and 1.2 for phases A, B and C, respectively.

Computational simulations were conducted using the *Matlab R2018a* toolbox *Intlab* [28], which is a useful instrument to deal with real and complex interval scalars, vectors and matrices. A given tolerance of $\tau = 1 \times 10^{-6}$ is used for the computational simulations in this paper and the Krawczyk operator is applied three times, since an angular displacement of $\Delta\omega_R = 120°$ is adopted. All calculations were performed in a *Intel Core i7-5500 @ 2.41GHz* processor.
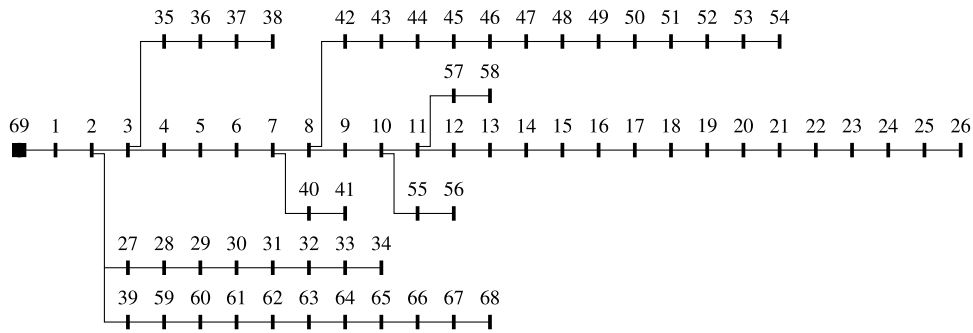
Fig. 2. IEEE 69-bus test system.

(a) $|V^A|$
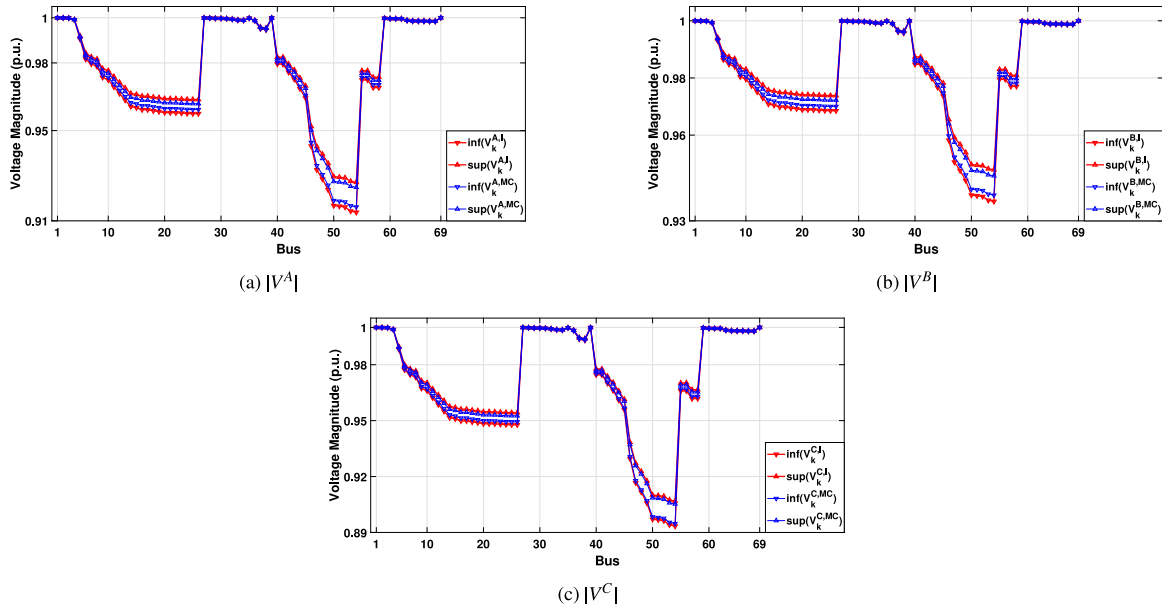
(b) $|V^B|$

(c) $|V^C|$

Fig. 3. Interval voltage magnitudes obtained with ITPCIM (red) and MCS (blue) in IEEE 69-bus distribution system for a 5% load uncertainty. (For interpretation of the references to colour in this figure legend, the reader is referred to the web version of this article.)

3.1. Applicability of ITPCIM

To check the applicability of the developed interval methodology, the results obtained with the application of ITPCIM are compared with the ranges of values obtained with the MCS probabilistic method. Figs. 3 and 4 show, respectively, the magnitude and angle intervals of the three-phase voltages in each bus for the IEEE 69-bus system considering a 5% load uncertainty. The red curves represent the limits of the intervals obtained with IPTCIM and the blue curves represent the limits obtained with MCS.

As can be noted in Figs. 3 and 4, the intervals obtained with the developed methodology encompass the possible results obtained with MCS, suggesting that the ITPCIM method is applicable in the calculation of the three-phase interval power flow. A quantitative analysis of the results will be made next with a comparison between those interval representations and the verification of the effectiveness of the proposed improvements.

3.2. Comparative analysis

The objective of this section is to compare the voltages obtained in the three-phase interval power flow calculation considering the proposed improvements treating the variables in interval and affine form.

To compare the interval results, the evaluation indexes presented in [29] are used. Basically, those indexes determine the minimum, maximum and average percentage of agreement between an output obtained with the interval methodology and the true interval solution, represented by the limits obtained by MCS. Therefore, these evaluation indexes A_{min}, A_{max} and A described by Eqs. (26), (27) and (28) take into account the amount of an interval variable that involves the true solution of that variable.

$$A_{\min} = \min\left(\frac{\omega(X_k^{MC})}{\omega(X_k^I)}\right) \cdot 100\% \tag{26}$$

$$A_{\max} = \max\left(\frac{\omega(X_k^{MC})}{\omega(X_k^I)}\right) \cdot 100\% \tag{27}$$

$$A = \frac{\sum_{k=1}^n \omega(X_k^{MC})}{\sum_{k=1}^n \omega(X_k^I)} \cdot 100\% \tag{28}$$

where $\omega(X_k^{MC})$ is the width of possible values obtained with MCS for some variable at bus k and $\omega(X_k^I)$ is the width of this interval variable at bus k obtained with the application of some interval methodology. The closer to 100%, the greater the range that encompasses the true solution of this variable.

In addition to the representation using conventional interval arithmetic (IA), the representation of interval variables in the affine form is also used. Affine Arithmetic (AA), which is described in Appendix B has the advantage of dealing with the dependency problem in interval calculations and this feature can avoid overestimating results in many cases.
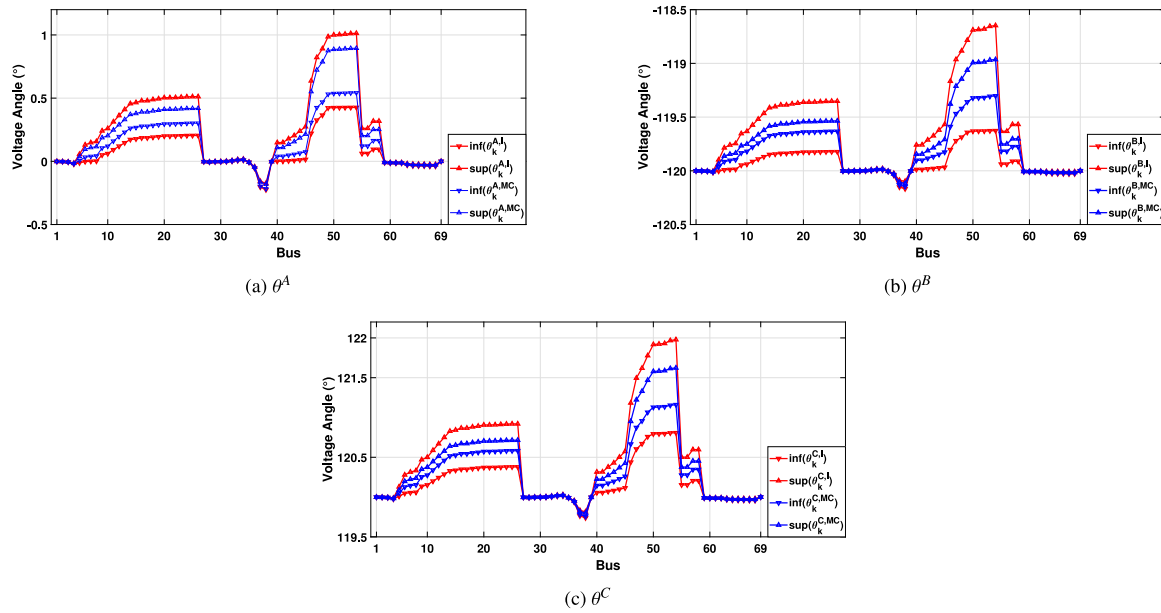
(a) θ^A

(b) θ^B

(c) θ^C

Fig. 4. Interval voltage angles obtained with ITPCIM (red) and MCS (blue) in IEEE 69-bus distribution system for a 5% load uncertainty. (For interpretation of the references to colour in this figure legend, the reader is referred to the web version of this article.)

Table 2
Evaluation indexes considering voltage magnitudes in each phase in IEEE 69-bus distribution system with level of uncertainty of 5%.

Method	Phase A			Phase B			Phase C		
	A_{min}	A_{max}	A	A_{min}	A_{max}	A	A_{min}	A_{max}	A
IA	16.91%	37.37%	26.87%	12.93%	28.54%	20.64%	19.09%	39.64%	28.14%
AA	34.58%	75.57%	50.87%	18.92%	41.73%	30.15%	27.99%	57.71%	41.15%
IA_{IE}	34.45%	75.56%	50.66%	18.86%	41.42%	30.03%	27.99%	57.71%	41.15%
AA_{IE}	34.56%	75.57%	50.82%	18.91%	41.67%	30.13%	27.99%	57.71%	41.15%
$ITPCIM_{IA}$	34.45%	75.56%	50.66%	31.92%	65.99%	47.50%	39.25%	78.53%	57.09%
$ITPCIM_{AA}$	34.56%	75.57%	50.82%	31.99%	66.00%	47.63%	39.38%	78.54%	57.10%

Table 3
Evaluation indexes considering voltage angles in each phase in IEEE 69-bus distribution system with level of uncertainty of 5%.

Method	Phase A			Phase B			Phase C		
	A_{min}	A_{max}	A	A_{min}	A_{max}	A	A_{min}	A_{max}	A
IA	37.86%	75.43%	49.52%	20.64%	43.49%	27.18%	24.55%	58.70%	34.24%
AA	38.04%	75.45%	49.82%	20.74%	43.50%	27.31%	24.55%	58.70%	34.24%
IA_{IE}	37.92%	75.44%	49.62%	20.66%	43.49%	27.21%	24.55%	58.70%	34.24%
AA_{IE}	38.02%	75.45%	49.77%	20.72%	43.50%	27.29%	24.55%	58.70%	34.24%
$ITPCIM_{IA}$	37.92%	75.44%	49.62%	20.66%	43.49%	27.21%	24.55%	58.70%	34.24%
$ITPCIM_{AA}$	38.02%	75.45%	49.77%	20.72%	43.50%	27.29%	24.55%	58.70%	34.24%

The results of IEEE 69-bus distribution system considering different interval approaches are shown in Table 2. In this table, IA and AA describe the results considering variables represented in interval arithmetic or affine arithmetic forms without applying any proposed improvement; IA_{IE} and AA_{IE} represent the use of the interval extension technique for these same interval representation forms; and $ITPCIM_{IA}$ and $ITPCIM_{AA}$ describe the use of all proposed improvements, considering IA and AA, respectively. Table 3 presents the evaluation index for the voltage angles. For all cases, the uncertainty level is 5%.

A simple analysis of Table 2 shows that as the proposed improvements are applied, there is a gradual improvement in the results. It is possible to observe a growth of the A_{min}, A_{max} and A indexes in the three phases with the application of ITPCIM, considering both interval and affine representation forms, which shows that the results obtained with the application of the proposed methodology are closer to the true

solution. Furthermore, Table 2 shows that the simple application of interval extensions in the IA representations considerably improves A_{min}, A_{max} and A, which are very close to the indexes obtained considering affine representation form.

It can also be seen in Table 2 that considering both the interval extensions and the angular rotation techniques in the application of ITPCIM, it is possible to observe a greater proximity of the indexes between the three phases. Although the indexes obtained with the use of interval extensions remain unchanged with the application of ITPCIM in phase A, there is a significant improvement in the results of phases B and C.

Table 3 shows that there is no change in the indexes obtained for voltage angles, regardless of the improvement applied or the form of interval representation used. For this reason, next evaluations will not be made based on this variable.

Table 4
Average time spent in IEEE 69-bus load flow calculation considering level of uncertainty of 5%.

Method	Average Time (s)	Standard Deviation (s)
MCS	2322.13	7.13
IA	9.06	0.04
AA	967,71	27.92
IA_{IE}	27.79	0.27
AA_{IE}	701.08	15.11
$ITPCIM_{IA}$	40.01	0.59
$ITPCIM_{AA}$	1808.09	21.01

As mentioned in Section 2.2.3, $\omega_R = 120°$ in the application of the angular rotation technique. It is observed that for the values of ω_R equal to 120°, 60° or 30° the solutions do not present significant changes. Furthermore, the results considering $\omega_R = 180°$ are practically identical to the results when the technique is not applied. Therefore, to avoid unnecessary computational effort and guarantee good results, $\omega_R = 120°$ is indicated.

Table 4 shows the mean and standard deviation values related to the computational time in seconds spent in MCS and the calculation of three-phase interval load flow considering the application of proposed improvements and the IA and AA forms of representation. The power flow of the IEEE 69-bus distribution system was calculated 10 times with each approach considering a 5% load uncertainty level.

It can be observed that, in general, the representation of the interval variables in the IA form requires significantly lower computational cost than MCS and AA form. Furthermore, to obtain practically the same results, the application of ITPCIM considering the AA form of representation takes on average about 45 times more seconds than IA form. When compared with MCS, $ITPCIM_{IA}$ takes about 58 times less seconds. A point related to the AA representation is that the use of interval extensions (represented by AA_{IE}) makes the interval load flow converge with less iterations to obtain practically the same results.

The proximity of the results obtained with $ITPCIM_{AA}$ and $ITPCIM_{IA}$ presented in Table 2 associated with the significant difference in computational cost shown in Table 4 are determining factors to establish that the results presented in next evaluations will only take into account the application of the developed methodology considering IA representation, being represented by ITPCIM.

3.3. ITPCIM analysis

The application of ITPCIM is evaluated considering different levels of load variation from three different unbalanced three-phase distribution systems: IEEE 69-bus, described in [27]; IEEE 13-bus, specified in [30]; and IEEE 33-bus, minutely detailed in [31].

Table 5 presents a complete analysis of the behaviour of the voltage magnitude indexes A_{min}, A_{max} and A for those three distribution systems with the application of ITPCIM considering load variations. The analysis is done for the three phases and the considered levels of load uncertainty are 5%, 7%, 10% and 15%.

The fact that the same evaluation index does not show significant variation with the increase in the load uncertainty level indicates that the intervals obtained with the ITPCIM vary practically in the same proportion to the true solution, which suggests that the increase in the uncertainty level on load did not result in overestimation in the magnitudes of the obtained interval voltages for any of the studied systems.

Although the results presented in Table 5 are interesting to evaluate the behaviour of ITPCIM in view of the variation in load, it is not possible to precisely quantify the width of the intervals obtained with ITPCIM. For that, it is possible to do the voltage sensitivity analysis, established in [18] and described by Eq. (29), which relates the width of the resulting voltage interval in a bus k with its deterministic value,

obtained without load variation. In addition, the voltage sensitivity indicates which buses in the system are most sensitive to the variations in which they are subjected.

$$S_{V_k}^{\%,s} = \frac{\omega(V_k^{i,s})}{V_k^{d,s}} \cdot 100\% \qquad (29)$$

Based on Eq. (29), the greater the percentage voltage sensitivity $S_{V_k}^{\%,s}$, the greater the width of the interval in relation to the deterministic variable it represents. Therefore it is interesting that $S_{V_k}^{\%,s}$ be as small as possible.

Fig. 5 shows the three-phase percentage voltage sensitivity between intervals obtained with the application of conventional interval arithmetic and ITPCIM in three different distribution systems considering a 5% variation in demand. The continuous lines denoted by $S_{V_{IA}}^{\%,s}$ represent the application of conventional interval arithmetic while the dotted lines represent voltage sensitivity using ITPCIM and it is denoted by $S_{V_{ITPCIM}}^{\%,s}$, where $s = A, B, C$.

As presented in Fig. 5, there is a decrease in the percentage voltage sensitivity with the application of ITPCIM in the three studied distribution systems. For certain phases of some systems, this reduction is greater than 50%, indicating that the width of the interval has been reduced by half in most cases with the application of the proposed improvements.

Therefore, the analysis of Fig. 5 and Table 2 suggests that the use of interval extensions and the application of angular rotation technique not only reduce the width of the intervals, but also increase the portion of the interval that corresponds to the true solution.

The percentage sensitivity related to the angle of the voltage is not calculated in this work because Eq. (29) does not apply properly for phasors located very close to zero degrees, which is the case of most voltages in phase A.

For a more complete analysis, Table 6 shows the maximum ($S_{V_{max}}^{\%}$) and average values ($S_{V_{avg}}$) of percentage voltage sensitivity for the same systems studied in Table 5, considering the three phases and the same levels of load uncertainty.

Through the analysis of Table 6 it is possible to see in all the studied systems that as the level of load uncertainty grows, there is also an increase in the width of the voltage intervals and, consequently, in the percentage voltage sensitivity. Also, it is important to mention that Table 5 indicates that the increase in the width of the voltage intervals followed, in general, the growth in the range determined by the limits obtained with MCS.

Finally, the $S_{V_{avg}}$ index shows which distribution systems have bus subject to the bigger voltage variation of a given phase caused by load changes. Therefore, a simple analysis of Table 6 indicates that the voltages in IEEE 13-bus system are more subject to variation from load uncertainty than IEEE 33 and 69-bus systems.

3.4. Case study with distributed generation (DG)

This case study aims to analyse the impact of DG penetration on ITPCIM implementation. For this, DG units are considered in buses 26 and 54, located at the end of two branches of distribution system IEEE 69-bus (Fig. 2). The three-phase active power generation of a DG unit is considered equal to the active demand per phase of the bus on which the unit is located.

The results obtained with the application of ITPCIM are also compared with the ranges of values obtained with the MCS to check the applicability of the methodology developed in the case of DG units penetration. Figs. 6 and 7 show, respectively, the magnitude and angle intervals of the three-phase voltages in each bus for the IEEE 69-bus system considering a 5% load and generation uncertainty. The red curves represent the limits of the intervals obtained with IPTCIM and the blue curves represent the limits obtained with MCS.

As can be seen in Figs. 6 and 7, the intervals obtained with ITPCIM encompass the possible results obtained with MCS, suggesting that

Table 5
Evaluation indexes considering voltage magnitude in each phase in distribution systems.

System	Uncertainty	Phase A			Phase B			Phase C		
		A_{min}	A_{max}	A	A_{min}	A_{max}	A	A_{min}	A_{max}	A
IEEE 13-bus	5%	50.34%	54.48%	51.10%	39.46%	40.84%	40.00%	48.76%	51.78%	49.50%
	7%	50.69%	55.23%	51.59%	40.58%	42.14%	41.25%	48.76%	51.86%	49.39%
	10%	48.93%	53.28%	49.95%	38.88%	40.86%	39.62%	47.96%	51.22%	48.78%
	15%	52.00%	56.68%	53.10%	44.58%	46.58%	45.43%	52.44%	54.95%	53.17%
IEEE 33-bus	5%	41.56%	88.91%	53.41%	36.49%	43.30%	39.12%	37.02%	50.71%	44.55%
	7%	42.36%	86.75%	54.40%	33.81%	42.98%	38.18%	33.83%	50.85%	43.68%
	10%	44.42%	86.55%	53.32%	32.76%	40.77%	36.20%	35.59%	54.65%	46.81%
	15%	43.57%	86.21%	53.51%	30.63%	40.07%	35.18%	33.62%	52.17%	44.78%
IEEE 69-bus	5%	34.45%	75.56%	50.66%	31.92%	65.99%	47.50%	39.25%	78.53%	57.09%
	7%	34.14%	72.31%	50.18%	34.41%	68.28%	46.59%	36.73%	76.45%	57.29%
	10%	35.09%	70.40%	50.48%	33.02%	69.08%	46.91%	37.26%	77.67%	57.43%
	15%	34.88%	71.35%	50.20%	33.44%	67.10%	46.26%	36.62%	76.44%	57.69%

(a) IEEE 13-bus

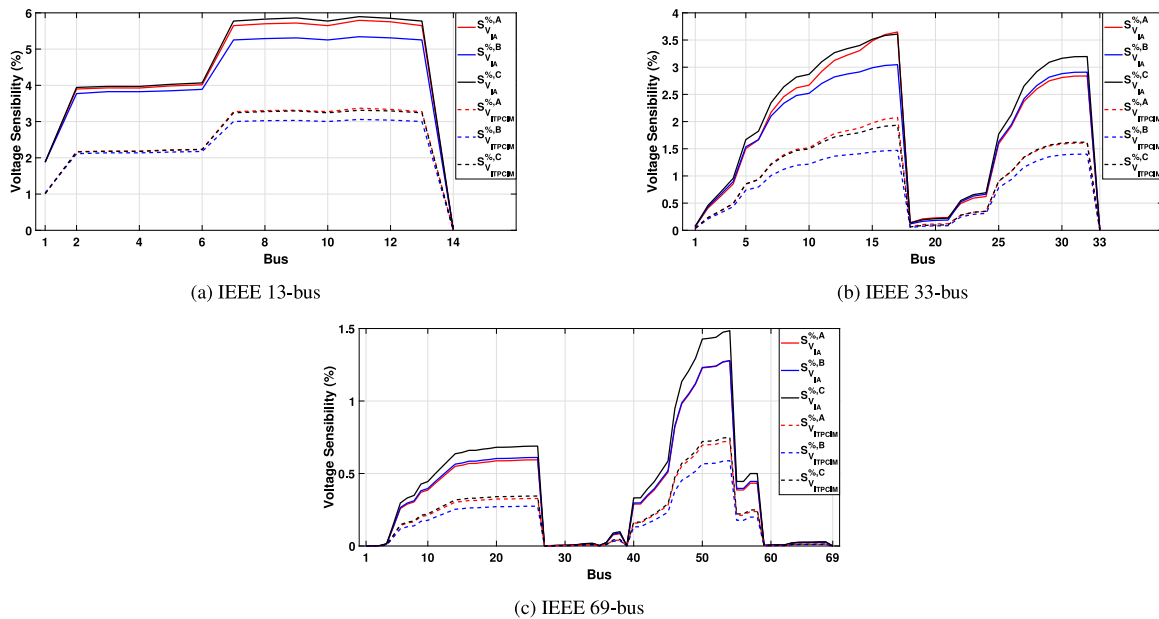(b) IEEE 33-bus

(c) IEEE 69-bus

Fig. 5. Percentage voltage sensitivity $S_{V_k}^{\%,s}$ obtained with conventional interval arithmetic (continuous lines) and ITPCIM (dotted lines) in three different distribution systems for a 5% load uncertainty.

Table 6
Voltage sensitivity in distribution systems with different levels of uncertainty.

System	Uncertainty	Phase A		Phase B		Phase C	
		$S_{V_{max}}^{\%}$	$S_{V_{avg}}$	$S_{V_{max}}^{\%}$	$S_{V_{avg}}$	$S_{V_{max}}^{\%}$	$S_{V_{avg}}$
IEEE 13-bus	5%	3.37%	2.51%	3.06%	2.35%	3.31%	2.49%
	7%	4.72%	3.51%	4.28%	3.29%	4.64%	3.49%
	10%	6.73%	5.02%	6.11%	4.70%	6.62%	4.98%
	15%	10.09%	7.52%	9.16%	7.05%	9.91%	7.46%
IEEE 33-bus	5%	2.08%	1.04%	1.47%	0.84%	1.93%	1.02%
	7%	2.91%	1.45%	2.11%	1.20%	2.71%	1.43%
	10%	4.16%	2.08%	3.13%	1.78%	3.88%	2.04%
	15%	6.25%	3.13%	5.04%	2.86%	5.84%	3.07%
IEEE 69-bus	5%	0.72%	0.20%	0.59%	0.17%	0.75%	0.21%
	7%	1.02%	0.29%	0.83%	0.24%	1.05%	0.30%
	10%	1.46%	0.41%	1.19%	0.34%	1.50%	0.42%
	15%	2.20%	0.62%	1.80%	0.51%	2.25%	0.64%

the developed methodology is applicable in the calculation of the three-phase interval power flow considering DG penetration.

For a more complete analysis of cases with DG penetration in IEEE 69-bus, the evaluation index A and the voltage perceptual sensitivity $S_{V_k}^{\%,s}$ are calculated and shown in Tables 7 and 8. The analyses are performed for the three phases and the considered levels of uncertainty are the same as those already explored in this work. However, uncertainty now affects both demand and generation.

The analysis of Table 7 shows that once again the same evaluation index does not undergo significant variation with the increase in the load and generation uncertainty levels, which indicates that the intervals obtained with the ITPCIM for the IEEE 69-bus vary practically at the same proportion to the true solution, suggesting that the increase in the uncertainty level of load and generation did not result in overestimation in the magnitudes of the obtained interval voltages. Furthermore, it can be noted that the indexes calculated with DG penetration have magnitudes close to those showed in Eq. (28), calculated disregarding the insertion of DG units.

The percentage voltage sensitivity levels indicated by Table 8 follow the same pattern as when DG units are not considered. It is possible to see in that as the level of load and generation uncertainty grows, there is also an increase in the width of the voltage intervals and, consequently, in the percentage voltage sensitivity.
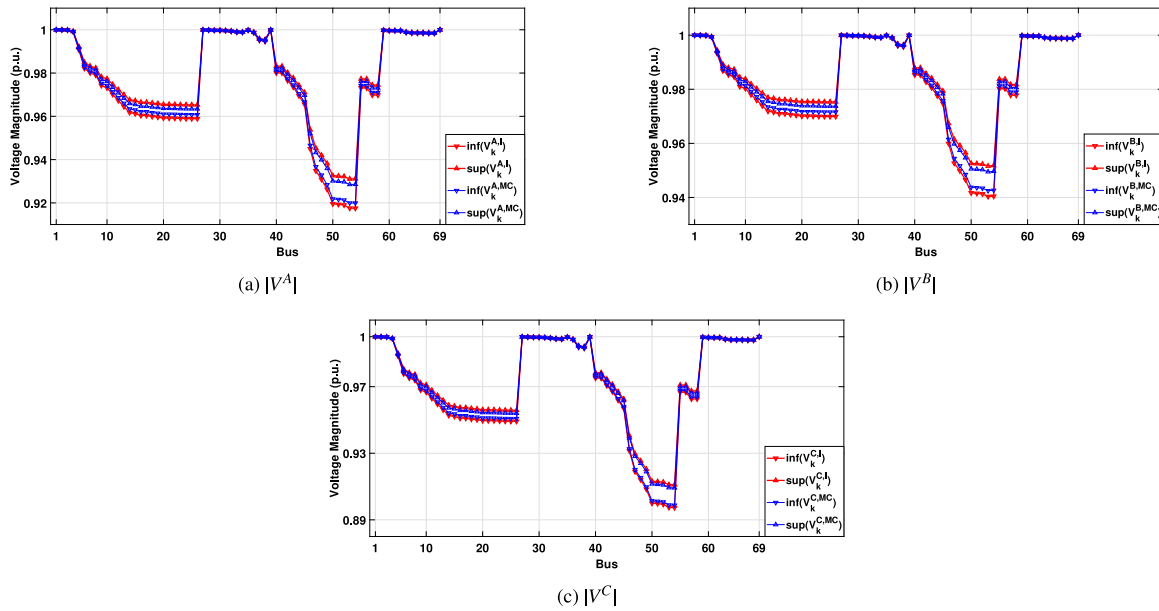
(a) $|V^A|$　　　　　　　　　　　(b) $|V^B|$

(c) $|V^C|$

Fig. 6. Interval voltage magnitudes obtained with ITPCIM (red) and MCS (blue) in modified IEEE 69-bus distribution system for a 5% load uncertainty. (For interpretation of the references to colour in this figure legend, the reader is referred to the web version of this article.)

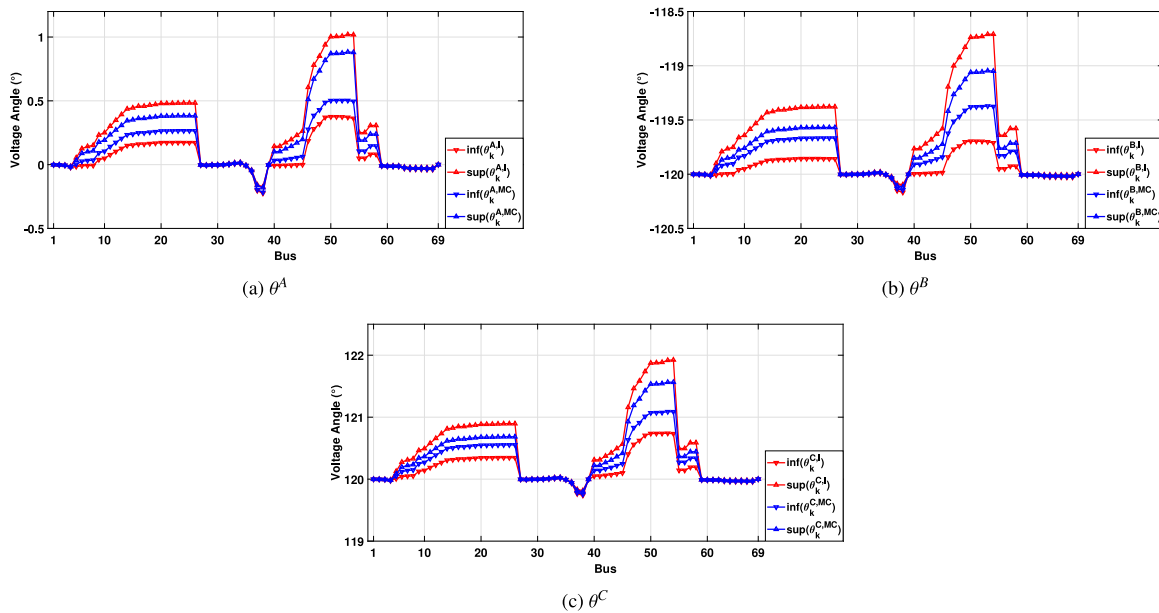(a) θ^A　　　　　　　　　　　(b) θ^B

(c) θ^C

Fig. 7. Interval voltage angles obtained with ITPCIM (red) and MCS (blue) in modified IEEE 69-bus distribution system for a 5% load and generation uncertainty. (For interpretation of the references to colour in this figure legend, the reader is referred to the web version of this article.)

Table 7
Evaluation indexes considering voltage magnitude in each phase at IEEE 69-bus with DG units allocated at buses 26 and 54.

Uncertainty	Phase A			Phase B			Phase C		
	A_{min}	A_{max}	A	A_{min}	A_{max}	A	A_{min}	A_{max}	A
5%	36.68%	73.12%	50.57%	34.95%	67.13%	48.24%	37.58%	76.75%	56.85%
7%	35.86%	72.12%	49.77%	32.38%	69.13%	46.69%	35.36%	75.95%	55.16%
10%	34.50%	72.61%	49.51%	32.35%	66.90%	46.21%	38.95%	74.91%	55.83%
15%	34.61%	70.42%	49.48%	34.24%	73.62%	47.67%	37.91%	76.95%	56.02%

Fig. 8 shows that applying the indicated improvements with ITPCIM in IEEE 69-bus also considerably reduces the percentage voltage sensitivity, indicating a considerable decrease in the width of obtained interval voltages.

It is important to mention that DG penetrations were tested for different locations and amounts of active power generation not only in the IEEE 69-bus but also in the other distribution systems studied in this paper. In all evaluations, the implementation of the ITPCIM method

Table 8
Voltage sensitivity in IEEE 69-bus considering DG units allocated at buses 26 and 54 for different levels of uncertainty.

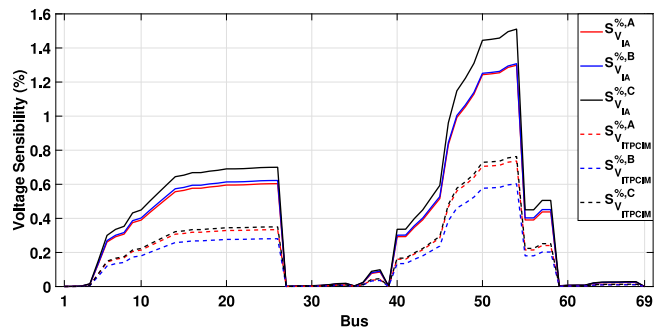| Uncertainty	Phase A		Phase B		Phase C	
	$S_{V_{max}}^{\%}$	$S_{V_{avg}}$	$S_{V_{max}}^{\%}$	$S_{V_{avg}}$	$S_{V_{max}}^{\%}$	$S_{V_{avg}}$
5%	0.74%	0.21%	0.60%	0.17%	0.76%	0.21%
7%	1.04%	0.29%	0.85%	0.24%	1.07%	0.30%
10%	1.49%	0.42%	1.22%	0.35%	1.53%	0.43%
15%	2.24%	0.63%	1.84%	0.52%	2.29%	0.64%

Fig. 8. Percentage voltage sensitivity $S_{V_k}^{\%,s}$ obtained with conventional interval arithmetic (continuous lines) and ITPCIM (dotted lines) in IEEE 69-bus considering GD units penetration at buses 26 and 54 for a 5% uncertainty in load and generation.

Table 9
Correlation analysis.

Uncertainty	Phase A		Phase B		Phase C	
	r_l	r_u	r_l	r_u	r_l	r_u
5%	0.9964	0.9935	0.9905	0.9742	0.9976	0.9969
7%	0.9965	0.9922	0.9919	0.9660	0.9976	0.9967
10%	0.9968	0.9900	0.9931	0.9414	0.9977	0.9961
15%	0.9968	0.9816	0.9951	0.9818	0.9972	0.9943

is relevant and there is no significant disparity in the obtained results. Due to limited space, these analyses were not included in this section.

A correlation analysis is proposed considering the results obtained using Eq. (30) in which N is the total number of buses of the system, V_l is the lower bound of the voltages obtained using Monte Carlo simulations and $\hat{V}_l$ are the corresponding values determined by the proposed method. Their corresponding average values are denoted by $\underline{V}$ and $\hat{V}$, respectively.

$$r_l = \frac{\sum_{l=1}^{N}(V_l - \underline{V})(\hat{V}_i - \hat{V})}{\sqrt{\sum_{l=1}^{N}(V_l - \underline{V})\sum_{l=1}^{N}(\hat{V}_l - \hat{V})}} \tag{30}$$

Analogously, the results can be evaluated for the upper bounds of the interval values, according to Eq. (31):

$$r_u = \frac{\sum_{u=1}^{N}(V_u - \underline{V})(\hat{V}_u - \hat{V})}{\sqrt{\sum_{u=1}^{N}(V_u - \underline{V})\sum_{u=1}^{N}(\hat{V}_u - \hat{V})}} \tag{31}$$

Table 9 presents the correlation analysis for all the system phases for the case study. It can be noted that the results obtained using the proposed method and the MC simulations are similar, being their correlation close to the unitary value.

3.5. Frequency droop equations

In [32], the frequency droop equations are introduced into the three phase current injection method assuming the system frequency in Hz (Hertz) as a state variable to be calculated. In this case, Eq. (32) is used for determining the droop characteristics of the generation units in which $P_{k,g}^s$ is the active power output of the generator, $P_{k,0}^s$ is the
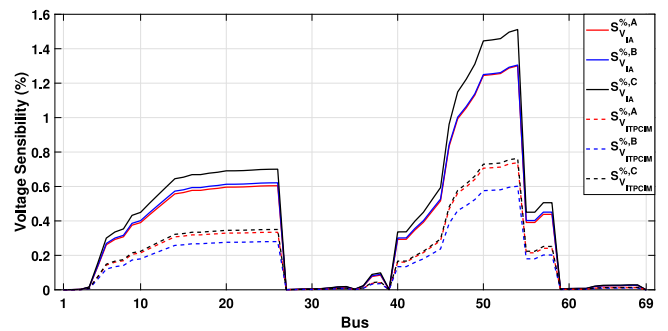

Fig. 9. IEEE 69-bus considering frequency droop control.

corresponding nominal value associated with the nominal frequency (f_0) and the f is the frequency value in Hertz to be determined by the algorithm.

$$P_{k,g}^s = P_{k,0}^s + K_f(f - f_0) \tag{32}$$

Note that the droop constant K_f is often referred to as the inverse of the generation unit statism and is generally less than 5% in the system base according to [32–34]. This constant may be associated mainly for rotating electrical machines and for Voltage Source Inverters (VSI) used for the connection of DG units into to distribution networks. The frequency variations are more expressive within microgrids environment due to the possibility of islanded operation [34]. However, it can be easily incorporated to the set of equations associated with the current injection method as described in [32] in order to calculate the system frequency.

It is important to notice that voltage control and frequency droop equations can be considered directly in the formation of the Jacobian matrix of the current injection method, as described in equations (A.15)-(A.19) in Appendix A, according to the original Ref. [32] in which this important contribution is presented. The proposed method consists on the application of the Krawczyk operator into the Jacobian matrix, being possible to obtain the results in this case.

New simulations are conducted in order to demonstrate the efficiency of the proposed method in this situation being the 69-bus test system used for the computational simulations of the case study described in Section 3.4. with the introduction of DG (Distributed Generation) units. The K_f droop constants of the generation units are set equal to 50 kW/Hz as adopted in [34] for the 69-bus test system.

Assuming an uncertainty of 5% associated with both load and generation data, the voltage sensitivities are given in percentage values in Fig. 9. Note that the values are similar to the ones obtained in the previous simulations and case studies.

Once the frequency value was considered as an additional variable to be calculated, it is important to present their values for different uncertainty percentage levels. In Table 10, the upper and lower limits of the frequency in Hertz are presented for different uncertainty values considering the results obtained from the Monte Carlo simulations and the proposed method in which the Krawczyk operator is applied into the Jacobian matrix.

It can be noted that similar results are obtained when compared to the traditional MC simulations, proving the efficiency and viability of the proposed method. The frequency variations are not expressive due to the connection of the substation (main energy source) to the distribution network as discussed in [34].

4. Conclusions

This paper presented a novel methodology for determining interval results of three-phase unbalanced power systems using the Three-Phase Current Injection Method (TPCIM) equations in which the state

Table 10
Interval analysis for frequency variation considering different uncertainty values.

Uncertainty	Monte Carlo		Proposed method	
	f_l	f_u	f_l	f_u
5%	59.9999	60.0001	59.9999	60.0001
7%	59.9999	60.0001	59.9999	60.0001
10%	59.9998	60.0002	59.9998	60.0002
15%	59.9997	60.0003	59.9997	60.0004

variables are considered in rectangular coordinates assuming intrinsic characteristics of distribution feeders such as radial topology, mutual impedances and unbalanced loads.

Based on the interval arithmetic, uncertainties are associated to active/reactive power injections at each system bus in order to evaluate their impact on the voltage magnitudes and angles.

In order to avoid Jacobian matrix inversion, the Krawczyk operator is applied into the power flow equations in order to obtain accurate interval solutions which can be compared to Monte Carlo simulations.

To validate the proposed methodology, different case studies are evaluated considering 13, 33 and 69 bus test systems. Results are compared with Monte Carlo solution and Affine Arithmetic results based on sensitivity analysis. Based on the simulations, it is possible to demonstrate that Monte Carlo solutions are accommodated between the limits obtained using the proposed method.

The analysis of presented results suggests that the use of interval extensions and the application of angular rotation technique not only reduce the width of the intervals, but also increase the portion of the interval that corresponds to the true solution.

Additionally, droop control and correlation analysis were performed in order to validate the proposed method to be used in distribution networks.

The method is useful for power distribution systems operation and planning studies, representing a viable and useful tool for calculating the impact of uncertain input data on the power flow results. Similar solutions are obtained when compared with Affine Arithmetic and Monte Carlo Simulations. Additionally, the computational time associated to the algorithm is extremely advantageous.

CRediT authorship contribution statement

Heitor M. Rodrigues Junior: Conceptualisation, Data curation, Writing - review & editing, Software, Visualisation. **Igor D. Melo:** Conceptualisation, Supervision, Methodology, Software, Writing - review & editing. **Erivelton G. Nepomuceno:** Supervision, Methodology, Writing - review & editing.

Declaration of competing interest

The authors declare that they have no known competing financial interests or personal relationships that could have appeared to influence the work reported in this paper.

Acknowledgements

Appendix A. Three-phase current injection method

The three-phase current injection method (TPCIM) is presented in [26]. It represents a novel formulation for the traditional power flow algorithm in which active and reactive powers are calculated as function of voltage magnitudes and angles in polar coordinates. TPCIM is formulated based on equations of calculated current injections expressed in terms of bus voltages in rectangular coordinates (real and imaginary parts).

Based on Eq. (A.1), it is possible to split the nodal current $\dot{I}_k^s$ into real and imaginary parts as presented by Eqs. (A.2) and (A.3):

$$\dot{I}_k^s = \frac{(P_k^{sch})^s - j(Q_k^{sch})^s}{(V_k^s)^*} \tag{A.1}$$

$$I_{re_k}^s = \frac{P_k^{sch,s} V_{re_k}^s + Q_k^{sch,s} V_{im_k}^s}{(V_{re_k}^s)^2 + (V_{im_k}^s)^2} \tag{A.2}$$

$$I_{im_k}^s = \frac{P_k^{sch,s} V_{im_k}^s - Q_k^{sch,s} V_{re_k}^s}{(V_{re_k}^s)^2 + (V_{im_k}^s)^2} \tag{A.3}$$

It is also possible to calculate the current injection vector $\underline{I}^{abc}$ according to the system (A.4) in which Y^{abc} is the admittance matrix incorporating the admittances of the network and $\underline{V}^{abc}$ is the voltage vector.

$$\underline{I}^{abc} = Y^{abc} \underline{V}^{abc} \tag{A.4}$$

It is possible to write the equation in rectangular coordinates (divided into real and imaginary parts) as presented by Eq. (A.5) and the matrix system (A.6) to be solved by direct method.

$$\underline{I_{re}}^{abc} + j\underline{I_{im}}^{abc} = (G^{abc} + jB^{abc})(\underline{V_{re}}^{abc} + j\underline{V_{im}}^{abc}) \tag{A.5}$$

$$\begin{bmatrix} \underline{I_{im}}^{abc} \\ \underline{I_{re}}^{abc} \end{bmatrix} = \begin{bmatrix} B^{abc} & G^{abc} \\ G^{abc} & -B^{abc} \end{bmatrix} \begin{bmatrix} \underline{V_{re}}^{abc} \\ \underline{V_{im}}^{abc} \end{bmatrix} \tag{A.6}$$

It is possible to calculate real and imaginary parts of the nodal injected current as respectively presented by (A.7) and (A.8).

$$I_{re_k}^s = \sum_{m \in \Omega_k} \sum_{t \in \varphi_p} (G_{km}^{st} V_{re_m}^t - B_{km}^{st} V_{im_m}^t) \tag{A.7}$$

$$I_{im_k}^s = \sum_{m \in \Omega_k} \sum_{t \in \varphi_p} (G_{km}^{st} V_{im_i}^t + B_{km}^{st} V_{re_m}^t) \tag{A.8}$$

where $s, t \in \varphi_p$ and $\varphi_p = \{a, b, c\}$. The index Ω_k represents the set of buses directly connected to bus k.

The difference between the calculated real and imaginary currents and their corresponding scheduled values in (A.2) and (A.3) must be equal to zero, as expressed by (A.9), (A.10), (A.11) and (A.12).

$$\Delta I_{re_k}^s = 0 \tag{A.9}$$

$$\Delta I_{im_k}^s = 0 \tag{A.10}$$

$$\frac{P_k^{sch,s} V_{re_k}^s + Q_k^{sch,s} V_{im_k}^s}{(V_{re_k}^s)^2 + (V_{im_k}^s)^2} - \sum_{m \in \Omega_k} \sum_{t \in \varphi_p} (G_{km}^{st} V_{re_m}^t - B_{km}^{st} V_{im_m}^t) = 0 \tag{A.11}$$

$$\frac{P_k^{sch,s} V_{im_k}^s - Q_k^{sch,s} V_{re_k}^s}{(V_{re_k}^s)^2 + (V_{im_k}^s)^2} - \sum_{m \in \Omega_k} \sum_{t \in \varphi_p} (G_{km}^{st} V_{im_i}^t + B_{km}^{st} V_{re_m}^t) = 0 \tag{A.12}$$

Once the system contains non linear equations, the solution is obtained iteratively by Newton–Raphson method as presented by (A.13):

$$\begin{bmatrix} \Delta \underline{I^a_{im}} \\ \Delta \underline{I^b_{im}} \\ \Delta \underline{I^c_{im}} \\ \Delta \underline{I^a_{re}} \\ \Delta \underline{I^b_{re}} \\ \Delta \underline{I^c_{re}} \end{bmatrix} = - \begin{bmatrix} \frac{\partial \underline{I^a_{im}}}{\partial \underline{V^a_{re}}} & \frac{\partial \underline{I^a_{im}}}{\partial \underline{V^b_{re}}} & \frac{\partial \underline{I^a_{im}}}{\partial \underline{V^c_{re}}} & \frac{\partial \underline{I^a_{im}}}{\partial \underline{V^a_{im}}} & \frac{\partial \underline{I^a_{im}}}{\partial \underline{V^b_{im}}} & \frac{\partial \underline{I^a_{im}}}{\partial \underline{V^c_{im}}} \\ \frac{\partial \underline{I^b_{im}}}{\partial \underline{V^a_{re}}} & \frac{\partial \underline{I^b_{im}}}{\partial \underline{V^b_{re}}} & \frac{\partial \underline{I^b_{im}}}{\partial \underline{V^c_{re}}} & \frac{\partial \underline{I^b_{im}}}{\partial \underline{V^a_{im}}} & \frac{\partial \underline{I^b_{im}}}{\partial \underline{V^b_{im}}} & \frac{\partial \underline{I^b_{im}}}{\partial \underline{V^c_{im}}} \\ \frac{\partial \underline{I^c_{im}}}{\partial \underline{V^a_{re}}} & \frac{\partial \underline{I^c_{im}}}{\partial \underline{V^b_{re}}} & \frac{\partial \underline{I^c_{im}}}{\partial \underline{V^c_{re}}} & \frac{\partial \underline{I^c_{im}}}{\partial \underline{V^a_{im}}} & \frac{\partial \underline{I^c_{im}}}{\partial \underline{V^b_{im}}} & \frac{\partial \underline{I^c_{im}}}{\partial \underline{V^c_{im}}} \\ \frac{\partial \underline{I^a_{re}}}{\partial \underline{V^a_{re}}} & \frac{\partial \underline{I^a_{re}}}{\partial \underline{V^b_{re}}} & \frac{\partial \underline{I^a_{re}}}{\partial \underline{V^c_{re}}} & \frac{\partial \underline{I^a_{re}}}{\partial \underline{V^a_{im}}} & \frac{\partial \underline{I^a_{re}}}{\partial \underline{V^b_{im}}} & \frac{\partial \underline{I^a_{re}}}{\partial \underline{V^c_{im}}} \\ \frac{\partial \underline{I^b_{re}}}{\partial \underline{V^a_{re}}} & \frac{\partial \underline{I^b_{re}}}{\partial \underline{V^b_{re}}} & \frac{\partial \underline{I^b_{re}}}{\partial \underline{V^c_{re}}} & \frac{\partial \underline{I^b_{re}}}{\partial \underline{V^a_{im}}} & \frac{\partial \underline{I^b_{re}}}{\partial \underline{V^b_{im}}} & \frac{\partial \underline{I^b_{re}}}{\partial \underline{V^c_{im}}} \\ \frac{\partial \underline{I^c_{re}}}{\partial \underline{V^a_{re}}} & \frac{\partial \underline{I^c_{re}}}{\partial \underline{V^b_{re}}} & \frac{\partial \underline{I^c_{re}}}{\partial \underline{V^c_{re}}} & \frac{\partial \underline{I^c_{re}}}{\partial \underline{V^a_{im}}} & \frac{\partial \underline{I^c_{re}}}{\partial \underline{V^b_{im}}} & \frac{\partial \underline{I^c_{re}}}{\partial \underline{V^c_{im}}} \end{bmatrix} \begin{bmatrix} \Delta \underline{V^a_{re}} \\ \Delta \underline{V^b_{re}} \\ \Delta \underline{V^c_{re}} \\ \Delta \underline{V^a_{im}} \\ \Delta \underline{V^b_{im}} \\ \Delta \underline{V^c_{im}} \end{bmatrix}$$

$$(A.13)$$

In compact form, the matrix system represented in (A.13) can be rewritten as presented in (A.14) in which the Jacobian matrix, J_{acob} contains all the partial derivatives associated with the problem.

$$\begin{bmatrix} \Delta \underline{I^{abc}_{im}} \\ \Delta \underline{I^{abc}_{re}} \end{bmatrix} = - \begin{bmatrix} J_{acob} \end{bmatrix} \begin{bmatrix} \Delta \underline{V^{abc}_{re}} \\ \Delta \underline{V^{abc}_{im}} \end{bmatrix} \qquad (A.14)$$

As described in [26], voltage control can be incorporated to the set of TPCIM equations in order to determine the reactive power output from generation buses to control the voltage magnitude at a given bus k' of the network, according to system represented in (A.15) where $\Delta \underline{Q^{abc}_{k'}}$ is associated with the three-phase reactive power calculated to control the voltage magnitude, denoted by $\underline{V^{abc}_{k'}}$.

Additionally, the droop control characteristics associated with primary frequency control, as determined by Eq. (32) can be easily incorporated to the set of equations according to [32]. In this case, the frequency f is added as variable to be determined by the load flow being associated with the reference angle θ_{ref} which is generally adopted as zero. Note that, in this formulation, any load bus can be adopted as angular reference for the system, being a particular contribution from the original methodology proposed in [32].

$$\begin{bmatrix} \Delta \underline{I^{abc}_{im}} \\ \Delta \underline{I^{abc}_{re}} \\ \Delta \underline{V^{abc}_{k'}} \\ \Delta \underline{\theta_{ref}} \end{bmatrix} = - \begin{bmatrix} J'_{acob} \end{bmatrix} \begin{bmatrix} \Delta \underline{V^{abc}_{re}} \\ \Delta \underline{V^{abc}_{im}} \\ \Delta \underline{Q^{abc}_{k'}} \\ \Delta f \end{bmatrix} \qquad (A.15)$$

The solution is obtained by Newton–Raphson iterative method being the solution updated at each iteration h as described in Eq. (A.16), (A.17), (A.18) and (A.19):

$$\left(\underline{V^{abc}_{re_k}} \right)^{(h+1)} = \left(\underline{V^{abc}_{re_k}} \right)^{(h)} + \left(\Delta \underline{V^{abc}_{re_k}} \right)^{(h)} \qquad (A.16)$$

$$\left(\underline{V^{abc}_{im_k}} \right)^{(h+1)} = \left(\underline{V^{abc}_{im_k}} \right)^{(h)} + \left(\Delta \underline{V^{abc}_{im_k}} \right)^{(h)} \qquad (A.17)$$

$$\left(\underline{Q^{abc}_{k'}} \right)^{(h+1)} = \left(\underline{Q^{abc}_{k'}} \right)^{(h)} + \left(\Delta \underline{Q^{abc}_{k'}} \right)^{(h)} \qquad (A.18)$$

$$f^{(h+1)} = f^{(h)} + \Delta f^{(h)} \qquad (A.19)$$

Appendix B. Affine arithmetic

Affine Arithmetic (AA) is a model for self-validated numerical computation that is similar to standard Interval Arithmetic, with the advantage that AA deals with the dependency problem in interval calculations. Thereby, AA tracks first-order correlations between input and computed quantities. In many cases, this feature can avoid overestimating results [35].

In AA, a partially unknown quantity x is represented by an affine form $\hat{x}$ which is described by the following first degree polynomial:

$$\hat{x} = x_0 + x_1 \epsilon_1 + x_2 \epsilon_2 + \cdots + + x_n \epsilon_n \qquad (B.1)$$

where x_0 is defined as the central value of $\hat{x}$ and x_i are real coefficients that represent partial deviations which depicts the magnitude of the corresponding uncertainty. The noise variables $\epsilon_i \in [-1, 1]$ represent independent components of the total quantity uncertainty x.

In AA, the same noise variable can contribute to the uncertainty of two or more computed quantities. Thus, if two affine forms $\hat{x}$ and $\hat{y}$ share the same noise symbol ϵ_i, there is a partial dependency between the quantities x and y. The coefficients x_i and y_i define the direction of this correlation.

Let $z = f(x, y)$ be a general operation. If f represents an affine operation, then $\hat{z}$ can be written as an affine combination of the noises ϵ_i. Thus, given two affine forms $\hat{x}$ and $\hat{y}$ and three real numbers α, β and γ, we have

$$\alpha \hat{x} + \beta \hat{y} + \gamma = (\alpha x_0 + \beta y_0 + \gamma) + (\alpha x_1 + \beta y_1) \epsilon_1 + \cdots + (\alpha x_n + \beta y_n) \epsilon_n \qquad (B.2)$$

Otherwise, if f represents a non-affine operation $\hat{z}$ cannot be strictly expressed as an affine combination of the noise symbols ϵ_i. According [36], this cases require that good affine approximation to exact solution must be used and an extra term to limit the error of this approach must be inserted.

References

[1] Karimi M, Mokhlis H, Naidu K, Uddin S, Bakar A. Photovoltaic penetration issues and impacts in distribution network–A review. Renew Sustain Energy Rev 2016;53:594–605.

[2] Mazhari SM, Monsef H, Romero R. A multi-objective distribution system expansion planning incorporating customer choices on reliability. IEEE Trans Power Syst 2015;31(2):1330–40.

[3] Liao X, Liu K, Le J, Zhu S, Huai Q, Li B, et al. Extended affine arithmetic-based global sensitivity analysis for power flow with uncertainties. Int J Electr Power Energy Syst 2020;115:105440.

[4] de Oliveira BC, Pereira JL, Alves GdO, Melo ID, de Souza MA, Garcia PA. Decentralized three-phase distribution system static state estimation based on phasor measurement units. Electr Power Syst Res 2018;160:327–36.

[5] Xu X, Yan Z. Probabilistic load flow calculation with quasi-Monte Carlo and multiple linear regression. Int J Electr Power Energy Syst 2017;88:1–12.

[6] Lin W, Yang Z, Yu J, Bao S, Dai W. Toward fast calculation of probabilistic optimal power flow. IEEE Trans Power Syst 2019;34(4):3286–8.

[7] Gruosso G, Maffezzoni P, Zhang Z, Daniel L. Probabilistic load flow methodology for distribution networks including loads uncertainty. Int J Electr Power Energy Syst 2019;106:392–400.

[8] Kalesar BM, Seifi AR. Fuzzy load flow in balanced and unbalanced radial distribution systems incorporating composite load model. Int J Electr Power Energy Syst 2010;32(1):17–23.

[9] Pourahmadi-Nakhli M, Seifi AR, Taghavi R. A nonlinear-hybrid fuzzy/probabilistic load flow for radial distribution systems. Int J Electr Power Energy Syst 2013;47:69–77.

[10] Albatsh FM, Mekhilef S, Ahmad S, Mokhlis H. Fuzzy-logic-based UPFC and laboratory prototype validation for dynamic power flow control in transmission lines. IEEE Trans Ind Electron 2017;64(12):9538–48.

[11] Gu W, Luo L, Ding T, Meng X, Sheng W. An affine arithmetic-based algorithm for radial distribution system power flow with uncertainties. Int J Electr Power Energy Syst 2014;58:242–5.

[12] Zhang C, Chen H, Guo M, Wang X, Liu Y, Hua D. DC power flow analysis incorporating interval input data and network parameters through the optimizing-scenarios method. Int J Electr Power Energy Syst 2018;96:380–9.

[13] Raj V, Kumar BK. A modified affine arithmetic-based power flow analysis for radial distribution system with uncertainty. Int J Electr Power Energy Syst 2019;107:395–402.

[14] Wang S, Dong Y, Wu L, Yan B. Interval overvoltage risk based PV hosting capacity evaluation considering PV and load uncertainties. IEEE Trans Smart Grid 2019.

[15] Liao X, Liu K, Zhang Y, Wang K, Qin L. Interval method for uncertain power flow analysis based on taylor inclusion function. IET Gener Transm Distrib 2017;11(5):1270–8.

[16] da Costa VM, Martins N, Pereira JLR. Developments in the NewtonRaphson power flow formulation based on current injections. IEEE Trans Power Syst 1999;14(4):1320–6.

[17] Pereira LES, da Costa VM, Rosa ALS. Interval arithmetic in current injection power flow analysis. Int J Electr Power Energy Syst 2012;43(1):1106–13.

[18] Araujo B, da Costa V. New developments in the interval current injection power flow formulation. IEEE Lat Am Trans 2018;16(7):1969–76.

[19] Ruback RO, Medeiros BS, et al. A new method for analyzing unsymmetrical faults under data uncertainties. Int J Electr Power Energy Syst 2018;102:38–51.

[20] Das B. Consideration of input parameter uncertainties in load flow solution of three-phase unbalanced radial distribution system. IEEE Trans Power Syst 2006;21(3):1088–95.

[21] Wang Y, Wu Z, Dou X, Hu M, Xu Y. Interval power flow analysis via multi-stage affine arithmetic for unbalanced distribution network. Electr Power Syst Res 2017;142:1–8.

[22] Alves HN. An interval arithmetic-based power flow algorithm for radial distribution network with distributed generation. J. Control, Automa Electr Syst 2019;30(5):802–11.

[23] Moore RE, Kearfott RB, Cloud MJ. Introduction to interval analysis, vol. 110. Siam; 2009.

[24] Revol N. Introduction to the IEEE 1788-2015 standard for interval arithmetic. In: International workshop on numerical software verification. Springer; 2017, p. 14–21.

[25] Nepomuceno EG, Junior HMR, Martins SA, Perc M, Slavinec M. Interval computing periodic orbits of maps using a piecewise approach. Appl Math Comput 2018;336:67–75.

[26] Garcia PA, Pereira JLR, Carneiro S, da Costa VM, Martins N. Three-phase power flow calculations using the current injection method. IEEE Trans Power Syst 2000;15(2):508–14.

[27] Das B. Radial distribution system power flow using interval arithmetic. Int J Electr Power Energy Syst 2002;24(10):827–36. http://dx.doi.org/10.1016/S0142-0615(01)00092-8.

[28] Rump S. INTLAB - Interval laboratory. In: Csendes T, editor. Developments in reliable computing. Dordrecht: Kluwer Academic Publishers; 1999, p. 77–104.

[29] Leng S, Liu K, Ran X, Chen S, Zhang X. An affine arithmetic-based model of interval power flow with the correlated uncertainties in distribution system. IEEE Access 2020;8:60293–304.

[30] Kersting WH. Radial distribution test feeders. IEEE Trans Power Syst 1991;6(3):975–85.

[31] Melo ID, Pereira JL, Variz AM, Garcia PA. Harmonic state estimation for distribution networks using phasor measurement units. Electr Power Syst Res 2017;147:133–44.

[32] de Oliveira Alves G, Pereira JLR, Passos Filho JaA. A new unbalanced three-phase governor power flow formulation based on the current injections method. Int J Electr Power Energy Syst 2020;123:106184.

[33] La Gatta PO, Passos Filho JaA, Pereira JLR. Tools for handling steady-state under-frequency regulation in isolated microgrids. IET Renew Power Gener 2019;13(4):609–17.

[34] de Sousa LL, Melo ID. Interval power flow analysis of microgrids with uncertainties: an approach using the second-order Taylor series expansion. Electr Eng 2021;1–11.

[35] de Figueiredo LH, Stolfi J. Affine arithmetic: concepts and applications. Numer Algorithms 2004;37(1–4):147–58.

[36] Pirnia M, Cañizares CA, Bhattacharya K, Vaccaro A. A novel affine arithmetic method to solve optimal power flow problems with uncertainties. IEEE Trans Power Syst 2014;29(6):2775–83.